Observational Study

Medicine®

OPEN

Analysis of the clinical manifestations and 18F-FDG PET-CT findings in 40 patients with histiocytic necrotizing lymphadenitis

Rui Zhang, MD, PhD[a], Lidan Liang, MD, PhD[b], Daoming Li, MD, PhD[c,*], Yuling Bai, MD[d], Xiangzhou Li, MD[e]

Abstract

Histiocytic necrotizing lymphadenitis (HNL) is a rare, benign, and self-limiting inflammatory disease that mainly involves the lymph nodes. There is a lack of large sample studies concerning the clinical manifestations and imaging features of 18F-fluorodeoxyglucose positron emission tomography/computed tomography (18F-FDG PET/CT) of HNL.

The clinical symptoms, laboratory examination results, 18F-FDG PET/CT imaging features, and treatment outcome were investigated in this retrospective study.

A total of 40 HNL patients were recruited. The onset age was between 14 and 65 years, with a median of 25 years. The white blood cell count was 3.9 (2.9, 7.1) $\times 10^9$/L, C-reactive protein level was 20.2 (6.6, 63.8) mg/L, erythrocyte sedimentation rate was 29.0 (18.0,45.0) mm/h, and ferritin was 616.5 (205.6, 2118.1) ng/mL. An abnormal liver function was observed in 23 patients. 18F-FDG PET-CT showed that an abnormal lymph node metabolism was observed in 38 patients, among which the highest 18F-FDG maximal standard uptake value (SUVmax) of the lymph nodes ranged between 3.4 and 41.9; the nodes were mainly distributed in the neck and axilla regions. Meanwhile, a total of 2502 lymph nodes (721 lymph nodes with a short axis greater than 10 mm) were found in the 38 patients, including 1837 lymph nodes with an 18F-FDG SUVmax $\geq$ 2.5. The 18F-FDG SUVmax of the spleen ranged from 2.5 to 9.2 in 20 patients, while that of central and peripheral bone marrow ranged from 2.7 to 36.0 in 30 patients. After follow-up for an average period of 1 month, the symptoms improved after prednisone treatment.

HNL often occurs in adolescents. Scanning with 18F-FDG PET/CT showed that most patients had multiple involved lymph nodes that were hypermetabolic, and only few lymph nodes are enlarged. Besides, the spleen or central and peripheral bone marrow could sometimes be hypermetabolic. Glucocorticoid treatment for the HNL patients is effective.

Abbreviations: 18F-FDG PET-CT = 18F-fluorodeoxyglucose positron emission tomography/computed tomography, CRP = C-reactive protein, EB = Epstein-Barr, ESR = erythrocyte sedimentation rate, HE = hematoxylin-eosin, HNL = histiocytic necrotizing lymphadenitis, LDH = lactate dehydrogenase, SUVmax = maximal standard uptake value.

Keywords: 18F-FDG PET-CT, clinical manifestations, histiocytic necrotizing lymphadenitis

1. Introduction

Histiocytic necrotizing lymphadenitis (HNL), also known as Kikuchi-Fujimoto disease or Kikuchi disease, was first described by the Japanese scholars Kikuchi and Fujimoto in 1972. This disease is a rare, benign, and self-limiting inflammatory disease that mainly involves the lymph nodes. The main clinical symptoms are fever and neck mass, and the natural course of the disease lasts 1 to 4 months. While most patients have good prognosis, the disease might reappear in a few patients.[1,2] Despite the global distribution of the disease, it has a certain geographical distribution, with a higher incidence rate in Asia, including China, Japan, and some Southeast Asian countries.[1,3–6] Due to the non-specific clinical manifestation, HNL patients are easily misdiagnosed with malignant lymphoma or tuberculosis.[7–9] 18F-fluorodeoxyglucose positron emission tomography/computed tomography (18F-FDG PET/CT) is an examination that integrates functional and anatomical images and has an important value in the diagnosis of tumors and inflammatory diseases.[10] Previous studies on the 18F-FDG PET/CT imaging characteristics of HNL mainly focused on case reports and small samples, which showed hypermetabolism in the lymph node lesions, but there is a lack of large sample studies to confirm that.[8,11–13] In order to further improve our understanding of HNL, we performed a retrospective study on the clinical data of HNL patients hospitalized in the First Affiliated Hospital of Zhengzhou University in China from January 2016

Editor: Subhashchandra Naik.

RZ and LL contributed equally to this work.

This work was supported by the Medical Science and Technology Research Program of Henan Province (No. LHGJ20190226).

The authors have no conflicts of interest to disclose.

The datasets generated during and/or analyzed during the current study are available from the corresponding author on reasonable request.

[a] Department of Respiratory and Critical Care Medicine, the First Affiliated Hospital of Zhengzhou University, Zhengzhou, China, [b] Department of Radiology, the First Affiliated Hospital of Zhengzhou University, Zhengzhou, China, [c] Department of Pathology, the First Affiliated Hospital of Zhengzhou University, Zhengzhou, China, [d] Emergency Intensive Care Unit, the First Affiliated Hospital of Zhengzhou University, Zhengzhou, China, [e] Department of Nuclear Medicine, the First Affiliated Hospital of Zhengzhou University, Zhengzhou, China.

[*] Correspondence: Daoming Li, The First Affiliated Hospital of Zhengzhou University, 1 East Jianshe Road, Zhengzhou, Henan 450052, China (e-mail: lidaoming@zzu.edu.cn).

How to cite this article: Zhang R, Liang L, Li D, Bai Y, Li X. Analysis of the clinical manifestations and 18F-FDG PET-CT findings in 40 patients with histiocytic necrotizing lymphadenitis. Medicine 2021;100:35(e27189).

Received: 18 February 2021 / Received in final form: 23 June 2021 / Accepted: 19 August 2021

http://dx.doi.org/10.1097/MD.0000000000027189

to June 2020, and summarized the clinical symptoms, laboratory examination results, 18F-FDG PET/CT imaging characteristics, and treatment outcomes of the patients.

2. Methods

2.1. Patients

HNL patients who were hospitalized in the First Affiliated Hospital of Zhengzhou University in China from January 2016 to June 2020 were recruited retrospectively. The inclusion criteria were as follows: HNL was diagnosed by the pathological examination of a lymph node biopsy. All patients had blood drawn for laboratory test at the first 24 hours after admission. 18F-FDG PET/CT was performed for each patient. The exclusion criteria were as follows: The patient had tuberculosis, lymphoma, cancer, or other diseases. The patient did not sign the informed consent. The study protocol was approved by the Ethics Committee of the First Affiliated Hospital of Zhengzhou University, and written informed consent was collected from the participants prior to the study (2020-KY-0211).

2.2. Laboratory examination

We used 5 mL of fasting intravenous blood with anti-coagulant to detect the blood routine, C-reactive protein (CRP), and erythrocyte sedimentation rate (ESR). In addition, 4 mL of venous blood in the procoagulant tube was centrifuged at 2500 rpm for 10 minutes, and serum was collected. An Olympus AU400 automatic biochemical analyzer (Olympus, Tokyo, Japan) was used to detect the biochemical indexes, including alanine aminotransferase, aspartate aminotransferase, gamma-glutamyl transpeptidase, alkaline phosphatase, and lactate dehydrogenase (LDH) according to the manufacturer's instructions. Meanwhile, a Roche automated immune analyzer (Roche diagnostics, Mannheim, Germany) was used to detect the serum ferritin level.

2.3. 18F-FDG PET/CT

All the patients underwent 18F-FDG PET/CT using a Siemens Biograph 64 TruePoint PET/CT scanner (Siemens healthcare, Germany). The patients were asked to fast for at least 6 hours before the 18F-FDG PET/CT scan and had glucose levels of less than 200 mg/dL. They received an intravenous injection of 0.1 to 0.12 mci/kg of 18F-FDG, and then they rested for 45 to 60 minutes in a prepared room. 64-slice CT was performed from the head to the pelvic floor, with 120 kV, 90 mA, and a section thickness of 3 mm, then a PET emission scan was immediately obtained in 3D mode. The PET data were iteratively reconstructed using the CT data for attenuation correction. Two nuclear medicine physicians with more than 10 years of experience evaluated the lesions of all patients according to the maximal standard uptake value (SUVmax). A lymph node was considered enlarged if its short axis was larger than 10 mm by the CT scan and hypermetabolic if its SUVmax $\geq$ 2.5. An 18F-FDG uptake exceeding 2.5 was considered abnormal.

2.4. Pathological examination

The biopsy specimens of the lymph nodes obtained by color Doppler ultrasound-guided or percutaneous CT-guided puncture were examined. Each specimen was fixed with 4% neutral formaldehyde solution, embedded in paraffin, sectioned at 4 μm and stained with hematoxylin-eosin (HE). The method of immunohistochemical staining was used to detect the markers of CD3, CD20, CD68, CD123, and MPO, and in situ hybridization was used to detect the expression level of Epstein-Barr (EB) virus. At the same time, with the patient in the lateral position on the platform bed, bone marrow puncture was performed, with the posterior superior iliac spine as the puncture point. Five bone marrow smears were prepared for the cell morphology examination.

2.5. Treatment outcome

A follow-up for an average of 1 month was performed on the patients, and the medication and treatment outcomes were observed.

2.6. Statistical analysis

Statistical analyses were performed using the SPSS 23.0 software (SPSS, Inc., Chicago, IL). Continuous variables were presented as mean $\pm$ SD or median (range), and categorical variables were presented as numbers and percentages.

3. Results

3.1. Clinical manifestations

A total of 40 patients with HNL were included in this study, among which 16 were males and 24 were females. The onset age was between 14 and 65 years, with a median age of 25 years. The course of disease lasted between 5 and 120 days, with a median of 15 days. The main symptoms included the following: fever (39 patients, 97.5%), neck mass (20 patients, 50.0%), headache (19 patients, 47.5%), myalgia (14 patients, 35.0%), fatigue (13 patients, 32.5%), cough (13 patients, 32.5%), sore throat (10 patients, 25.0%), rash (5 patients, 12.5%), expectoration (4 patients, 10%), abdominal pain (3 patients, 7.5%), nausea and (or) vomiting (3 patients, 7.5%), and diarrhea (1 patient, 2.5%). The clinical features of the 40 HNL patients in the study before treatment are shown in Table 1.

3.2. Laboratory examination

The detailed results of the laboratory examination in the 40 HNL patients before treatment are shown in Table 2. The values of the blood routine examination results were as follows: white blood cell count 3.9 (2.9, 7.1) $\times 10^9$/L, neutrophil count 2.1 (1.3, 4.0) $\times 10^9$/L, lymphocyte count 1.3 (0.9, 1.7) $\times 10^9$/L, hemoglobin (119.5 $\pm$ 16.5) g/L, and platelet count (184.8 $\pm$ 68.2) $\times 10^9$/L. CRP was 20.2 (6.6, 63.8) mg/L, ESR was 29.0 (18.0, 45.0) mm/h, and ferritin was 616.5 (205.6, 2118.1) ng/mL. The results of the biochemical parameters were as follows: alanine aminotransferase 27.2 (13.5, 51.5) U/L, aspartate aminotransferase 33.5 (22.3, 66.0) U/L, gamma-glutamyl transpeptidase 29.5 (16.3, 89.0) U/L, alkaline phosphatase 74.4 (53.3, 98.5) U/L, and LDH 367.0 (262.3, 536.8) U/L. An abnormal liver function was observed in 23 patients.

3.3. Imaging features of 18F-FDG PET/CT

Among the 40 patients, 2 patients had no lymph node enlargement or metabolism abnormality, and 38 patients had

Table 1

The clinical features of the 40 HNL patients in the study before treatment.

Clinical features	
Gender (number)	
Male	16
Female	24
Age (years)	14–65
(Median)	25
<18	7
18–20	5
>20–30	17
>30–40	6
>40	5
Duration (d)	15 (10,30)
Symptoms (number)	
Fever	39
38°C–39°C	12
≥39°C–40.5°C	27
Lymph node enlargement	38
Headache	19
Myalgia	14
Fatigue	13
Cough	13
Sore throat	10
Rash	5
Expectoration	4
Abdominal pain	3
Nausea/vomiting	3
Diarrhea	1
Complication (number)	
Hashimoto's thyroiditis	4
Systemic lupus erythematosus	1

One patient might have 1 or more symptoms.
HNL = histiocytic necrotizing.

Table 2

The results of the laboratory examination in the 40 HNL patients before treatment.

Laboratory examination	
Blood routine	
WBC count ($\times 10^9$/L)	3.9 (2.9, 7.1)
Leukopenia (<4×10^9/L)	20 (50%)
(4–10) × 10^9/L	15 (37.5%)
>10×10^9/L	5 (12.5%)
Neutrophil count ($\times 10^9$/L)	2.1 (1.3, 4.0)
Neutropenia (<1.5×10^9/L)	13 (32.5%)
Lymphocyte count ($\times 10^9$/L)	1.3 (0.9, 1.7)
Lymphopenia (<0.8×10^9/L)	7 (17.5%)
Hemoglobin (g/L)	119.5 ± 16.5
Platelet count ($\times 10^9$/L)	184.8 ± 68.2
CRP (mg/L)	20.2 (6.6, 63.8)
ESR (mm/h)	29.0 (18.0, 45.0)
Ferritin (ng/mL)	616.5 (205.6, 2118.1)
Liver function	
ALT (U/L)	27.2 (13.5, 51.5)
>40 U/L	16 (40%)
AST (U/L)	33.5 (22.3, 66.0)
>40 U/L	15 (37.5%)
γ-GT (U/L)	29.5 (16.3, 89.0)
>50 U/L	15 (37.5%)
ALP (U/L)	74.4 (53.3, 98.5)
>110 U/L	9 (22.5%)
LDH (U/L)	367.0 (262.3, 536.8)

The normal value range of the WBC count was (4–10) × 10^9/L. Leukopenia was defined as an absolute WBC count of less than 4×10^9/L. Neutropenia was defined as an absolute neutrophil count of less than 1.5×10^9/L. Lymphopenia was a lymphocyte count of less than 0.8×10^9/L. The normal value range of hemoglobin was (110–160) × 10^{12}/L, The normal value range of platelet count was (100–300) × 10^9/L. The increase in CRP was more than 10 mg/L. The increase in ESR was more than 15 mm/h. The normal value range of ferritin was (12–322) ng/mL. The normal value of ALT was less than 40 U/L. The normal value of AST was less than 40 U/L. The normal value of γ-GT was less than 50 U/L. The normal value of ALP was less than 110 U/L. The normal value range of LDH was 104 to 240 U/L.
Values were presented as mean ± SD or median (range) for continuous variables and as numbers (percentages) for categorical variables.
γ-GT = gamma-glutamyl transpeptidase, ALP = alkaline phosphatase, ALT = alanine aminotransferase, AST = aspartate aminotransferase, CRP = C-reactive protein, ESR = erythrocyte sedimentation rate, HNL = histiocytic necrotizing lymphadenitis, LDH = lactate dehydrogenase, WBC = white blood cell.

abnormal metabolism of the lymph nodes. Among these 38 patients, the highest 18F-FDG SUVmax of the lymph nodes was between 3.4 and 41.9, and these lymph nodes were mainly distributed in the neck in 26 patients (left: 16 patients, right: 10 patients), axilla in 6 patients (left: 2 patients, right: 4 patients), mediastinum in 3 patients, abdominal cavity in 1 patient, pelvic cavity in 1 patient, and right inguinal region in 1 patient (Each patient had only 1 lymph node with the highest 18F-FDG SUVmax). Table 3 shows the highest 18F-FDG SUVmax of the affected lymph nodes in 38 patients.

Meanwhile, a total of 2502 lymph nodes (including 721 lymph nodes with a short axis greater than 10 mm, accounting for 28.8%, and with the largest lymph node [25mm × 41 mm] being located in the mesenteric region) were found in the 38 patients. Among them, 1837 (73.4%) lymph nodes had an 18F-FDG SUVmax ≥ 2.5 and were distributed in the neck in 38 patients (bilateral neck: 33 patients, left neck: 2 patients, right neck: 3 patients), axilla in 26 patients (bilateral axilla: 17 patients, left axilla: 6 patients, right axilla: 3 patients), pulmonary hilar in 15 patients (bilateral hilar: 9 patients, left hilar: 3 patients, right hilar: 3 patients), abdominal cavity in 19 patients (retroperitoneum: 19 patients, mesenteric region: 4 patients, other regions: 12 patients), pelvic cavity in 17 patients (bilateral iliac region: 16 patients, right iliac region: 1 patient), mediastinum in 21 patients, chest wall in 8 patients, and bilateral inguinal region in 10 patients. The distribution of the 18F-FDG SUVmax of 1837 lymph nodes in 38 patients is shown in Table 4.

All the patients had no liver enlargement or metabolic abnormalities in the liver, while 29 patients (29/40) had splenic enlargement, among which 9 patients had normal spleen radioactivity distribution, and 20 patients had the 18F-FDG SUVmax of spleen ranging from 2.5 to 9.2. The 18F-FDG SUVmax of the central and peripheral bone marrow in 30 patients ranged from 2.7 to 36.0.

3.4. Pathological examination

The histopathological findings of the lymph nodes under HE staining included the subcapsular and subcortical areas of the lymph nodes, sometimes involving the cortex, with irregular patchy or piecemeal necrosis, obvious nuclear shrinkage or nuclear fragments in the necrotic foci. Besides, the findings showed proliferation of the different shapes of histiocytes, lymphocytes, and plasmacytoid dendritic cells around the necrotic foci, and no neutrophils infiltration around the necrotic areas was observed under the microscope. The results of the immunohistochemical staining showed that CD68 and MPO were positive in the proliferative histiocytes in all the patients, CD3 was positive in the T lymphocytes in 38 patients, CD68 and

Table 3

Detailed list of the highest 18F FDG SUVmax of the lymph nodes in 38 patients with HNL.

Location	The highest 18F-FDG SUVmax
Neck (median)	17.5
Left neck	6.5, 7.2, 7.6, 13, 13.6, 15.5, 16.4, 16.9, 18, 18.9, 21.4, 22.3, 24.2, 25.3, 29.9, 32.3
Right neck	8.5, 2.4, 12.9, 13.6, 14.9, 24.1, 24.4, 29.1, 33.3, 41.9
Axilla (median)	12.6
Left axilla	11.5, 13.7
Right axilla	3.4, 7.7, 16.6, 23.5
Mediastinum	14.1, 14.3, 19.1
Abdominal cavity	9.7
Pelvic cavity	19.4
Right inguinal region	19.1

Each patient had only 1 lymph node with the highest 18F-FDG SUVmax. HNL = histiocytic necrotizing, SUVmax = maximal standard uptake value.

CD123 were positive in the plasmacytoid dendritic cells in 35 patients, and CD20 was positive in the B lymphocytes of the lymphoid follicle in 34 patients. The results of in situ hybridization showed that all the samples tested negative for EB virus. The bone marrow smear showed active bone marrow hyperplasia, including the myeloid cells, erythroid cells, lymphocytes, and megakaryocytes, while the cell ratio and morphology were normal. The imaging features of 18F-FDG PET-CT and the HE pathological findings of 2 patients with fever are shown in Figures 1 and 2.

3.5. Treatment outcome

After the diagnosis was confirmed in all the patients, they received treatment with prednisone (0.5–1.0 mg/kg/d). The treatment course lasted 2 to 4 weeks, with a median of 22 days. One patient with persistent high fever of 39.6°C was given prednisone tablets (30 mg/d) after confirming the diagnosis, the treatment was regularly reduced by 1 tablet each week, and fever disappeared during this period. After 2 weeks, the fever reoccurred; then, the dosage was increased to 30 mg/d lasting for 16 days, and fever disappeared again.

4. Discussion

HNL is a non-neoplastic lymphadenitis disease, which is also known as pseudolymphoma-like hyperplasia. The onset age of the disease lies within a wide range, from 19 months to 75 years, but it is more common in adolescents.[14–17] The incidence rate of male to female is reported to be 1.0:2.8 to 1:4,[6,15–17] 1:1,[18,19] and rarely 1.8:1, occurring more easily in males.[13] This study showed the male to female ratio to be 1:1.5, suggesting that female patients are prone to the disease. The onset age was between 14 and 65 years, with a median of 25 years.

The pathogenesis of HNL is still unknown. While it has been reported to be related to viral infections, such as the EB virus, adenovirus, parvovirus B19, and human herpesvirus,[15,20,21] it may also be related to or be the precursor symptoms of autoimmune dysfunction, such as systemic lupus erythematosus, systemic sclerosis, Hashimoto thyroiditis, and other autoimmune diseases.[6,22] Besides, it may be related to physical and chemical factors.[23] This study showed that a few HNL patients were complicated with systemic lupus erythematosus or Hashimoto thyroiditis, which suggests that autoimmune dysfunction might be the cause of the disease in these patients.

The majority of HNL patients have fever, and some of them even have sustained high fever (39.1–40°C or >40°C), which might be accompanied by other symptoms like cough, sore throat, rash, nausea, vomiting, night sweats, weight loss, and others.[1,2] Meanwhile, HNL affects multiple lymph nodes, which might be distributed in the neck, axilla, inguinal region, mediastinum, pulmonary hilar, chest wall, abdominal cavity, and pelvic cavity, and sometimes the lesions involved the skin, liver, spleen, and bone marrow.[24,25] Laboratory examination showed decreased white blood cell and neutrophils counts and increased levels of CRP and ESR, accompanied by liver function damage and LDH increase in some of the patients.[26–28] The symptoms and results of the laboratory tests in HNL patients were consistent with the previous studies, but this study is the first to report elevated serum ferritin levels.

18F-FDG PET/CT is a non-invasive, non-traumatic whole-body imaging technology, which has an important role in diagnosing tumors and evaluating their stage and treatment outcome. Meanwhile, not only tumor cells can absorb 18F-FDG, but also inflammatory cells in infectious or non-infectious inflammatory sites, such as macrophages, neutrophils, and lymphocytes. Therefore, 18F-FDG PET/CT can also guide the diagnosis of inflammatory diseases and evaluation of the

Table 4

Distribution of the 18F-FDG SUVmax ≥ 2.5 of 1837 lymph nodes in 38 patients with HNL.

Distribution of 18F-FDG SUVmax ≥ 2.5 of lymph nodes (location and number of cases)					
Neck (38)	Axilla (26)	Pulmonary hilum (15)	Abdominal cavity (19)	Pelvic cavity (17)	Mediastinum (21)
Bilateral (33)	Bilateral (17)	Bilateral (9)	Retroperitoneum (19)	Bilateral iliac region (16)	Chest wall (8)
Left (2)	Left (6)	Left (3)	Mesenteric region (4)	Right iliac region (1)	Bilateral inguinal region (10)
Right (3)	Right (3)	Right (3)	Other regions (12)		

HNL = histiocytic necrotizing, SUVmax = maximal standard uptake value.

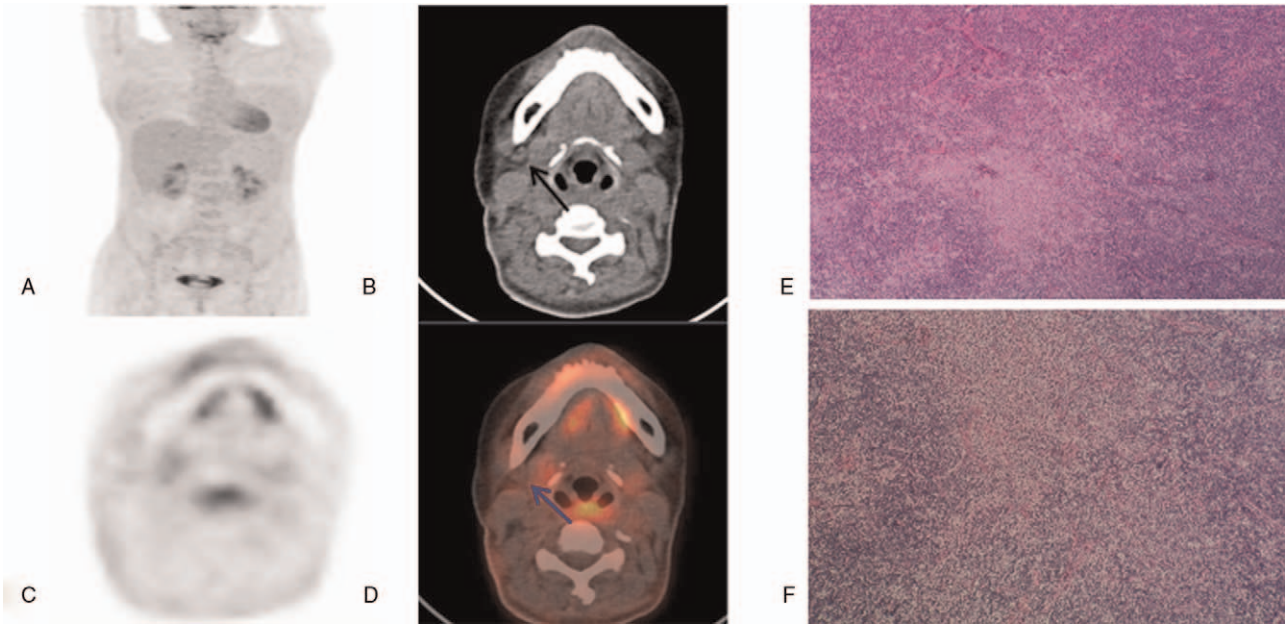

Figure 1. A 26-year-old female was admitted with fever for 10 days. 18F-FDG PET/CT (A) showed that all the lymph nodes had a short diameter less than 10 mm, and no metabolic abnormality of the lymph nodes in the whole body. CT (B) showed that the right cervical lymph node was 9.2 mm × 7.0 mm (arrow). PET (C) and PET/CT (D) showed no abnormal metabolism of the right cervical lymph node (arrow). Pathological results of the right cervical lymph node showed necrotizing lymphadenitis by HE staining (×40 times, E; ×100 times, F). 18F-FDG PET-CT = 18F-fluorodeoxyglucose positron emission tomography/computed tomography, HE = hematoxylin-eosin.

treatment outcome. Having SUVmax ≥ 2.5 is usually used as the criterion for malignant lesions. However, not much research has been done on whether this criterion is applicable to find involved lymph nodes in HNL patients. Using 18F-FDG PET/CT, Kong et al[13] found that among the 22 HNL patients in the study, 21 patients had cervical lymph nodes involved, 619 lymph nodes were hypermetabolic (SUVmax > 3.0), with a short axis less than 1 cm in 71.1% of them. This study showed that a total of 2502 lymph nodes (among which only 28.8% had a short axis greater than 10 mm) were found in the 38 patients, including 1837 lymph

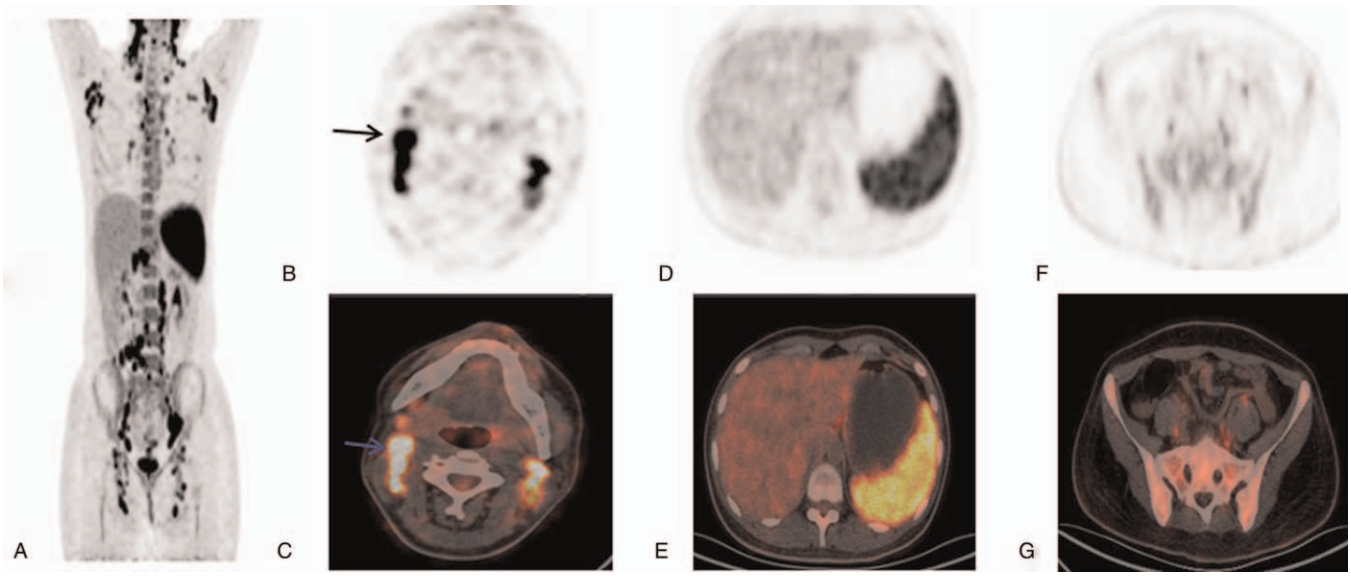

Figure 2. A 22-year-old female was admitted with fever for 12 days. 18F-FDG PET/CT (A) showed multiple hypermetabolic lymph nodes on both sides in the neck, bilateral axilla, mediastinum, pulmonary hilar, abdominal cavity, pelvic cavity, bilateral inguinal region, and central and peripheral bone marrow. PET (B) and PET/CT (C) showed bilateral hypermetabolic cervical lymph nodes and their fusion, and the 18F-FDG SUVmax of the lymph node (arrow) was 17.0. PET (D) and PET/CT (E) showed an increased splenic volume and spleen hypermetabolism, and the 18F-FDG SUVmax of the spleen was 10.2. PET (F) and PET/CT (G) showed slight hypermetabolism of the bilateral iliac bones, and the 18F-FDG SUVmax was 4.0. 18F-FDG PET-CT = 18F-fluorodeoxyglucose positron emission tomography/computed tomography, SUVmax = maximal standard uptake value.

nodes with an 18F-FDG SUVmax $\geq$ 2.5, which were mainly distributed in the neck and axilla regions. This suggests that the involved lymph nodes in most patients have hypermetabolism. While an 18F-FDG SUVmax $\geq$ 2.5 might be used as the criterion for involved lymph nodes in HNL patients, lymph node enlargement was found only in a few patients. Meanwhile, this study found a small number of patients with a normal metabolism or an 18F-FDG SUVmax $<$ 2.5 of the lymph nodes. The reason for this is not clear. Their diagnosis might be delayed or missed using 18F-FDG PET/CT scan, and it is necessary to perform lymph node biopsy. This study also showed that 50% (20/40) of the HNL patients had splenomegaly and spleen hypermetabolism, and 75% (30/40) of them had hypermetabolism of the central and peripheral bone marrow. The bone marrow smear showed active bone marrow hyperplasia in 40 patients, which could exclude hematological tumors. In addition, Murcia et al[29] reported that 18F-FDG PET/CT had an important value in the diagnosis of HNL and could also evaluate the curative effect of drugs on HNL.

The clinical symptoms and the results of the laboratory examination in HNL patients were not specific. While 18F-FDG PET/CT showed multiple hypermetabolic lymph nodes involved and played an important role in diagnosing HNL, the final diagnosis still needed to be confirmed through a lymph node biopsy. The pathological findings included coagulative necrosis in the paracortical area of the lymph nodes, sometimes involving the cortex. Nuclear shrinkage and nuclear fragment were seen in the core of the necrotic focus. The proliferation of histiocytes, lymphocytes, and plasmacytoid dendritic cells was mainly around the necrotic area. The above-mentioned pathological changes were consistent with what was reported in previous studies.[30,31] Chiu et al[32] detected the EB virus expression in the cytoplasmic apoptotic bodies of histiocytes and lymphocytes of HNL patients using the polymerase chain reaction. However, the hybridization signals of EB virus in the lymph nodes were not detected by in situ hybridization in this study, which indicates that it is still controversial to consider EB virus as the cause of HNL.

The drugs for HNL include glucocorticoid and non-steroidal anti-inflammatory drugs, but previous studies have shown that some patients can easily have a relapse after treatment.[33–35] In this study, all the patients were given prednisone treatment and all their symptoms disappeared, which suggests that the glucocorticoid treatment is effective.

However, some limitations of this study should be considered. Firstly, this single-sample study was conducted using a retrospective analysis. Secondly, it lacked a comparison of the laboratory examination and 18F-FDG PET/CT imaging findings before and after HNL treatment.

5. Conclusion

To sum up, HNL usually occurs in adolescents. The main clinical symptoms include fever and neck mass. Laboratory examination showed that some patients had leukopenia, neutropenia, and lymphopenia, while some had higher levels of CRP, ESR, ferritin, and LDH, which might be accompanied with liver function damage. Scanning with 18F-FDG PET/CT showed multiple involved lymph nodes with hypermetabolism in most patients, especially in the neck and axilla regions, only few enlarged lymph nodes and sometimes hypermetabolic spleen or central and peripheral bone marrow. However, a few patients had no abnormal metabolism of the lymph nodes. The diagnosis of HNL depends on the lymph node biopsy, and even a bone marrow biopsy is needed to exclude hematological diseases. The majority of HNL patients could improve after glucocorticoid treatment, but attention should be paid to the recurrence in the process of glucocorticoid reduction.

Acknowledgment

We thank EditSprings (https://www.editsprings.com) for its linguistic assistance during the preparation of this manuscript.

Author contributions

Conceptualization and design: RZ, LL and DL; provision of study materials or patients: RZ, LL, DL, YB and XL; collection and assembly of data: RZ, LL, DL, YB and XL; data analysis and interpretation: RZ, LL, DL, YB and XL; manuscript writing: all authors; final approval of manuscript: all authors.

Investigation: Rui Zhang, Lidan Liang, Daoming Li.

Writing – original draft: Rui Zhang, Lidan Liang, Daoming Li, Yuling Bai, Xiangzhou Li.

References

[1] Pileri S, Kikuchi M, Helbron D, Lennert K. Histiocytic necrotizing lymphadenitis without granulocytic infiltration. Virchows Arch A Pathol Anat Histol 1982;395:257–71.
[2] Bosch X, Guilabert A, Miquel R, Campo E. Enigmatic Kikuchi-Fujimoto disease: a comprehensive review. Am J Clin Pathol 2004;122:141–52.
[3] Suseelan AV, Augusty TS, Harilal KR. Necrotising lymphadenitis. An analysis of seventeen cases. Indian J Pathol Microbiol 1984;27:331–4.
[4] Dorfman RF. Histiocytic necrotizing lymphadenitis of Kikuchi and Fujimoto. Harefuah 1991;120:15–7.
[5] Kutty MK, Anim JT, Sowayan S. Histiocytic necrotising lymphadenitis (Kikuchi-Fujimoto disease) in Saudi Arabia. Trop Geogr Med 1991; 43:68–75.
[6] Dumas G, Prendki V, Haroche J, et al. Kikuchi-Fujimoto disease: retrospective study of 91 cases and review of the literature. Medicine (Baltimore) 2014;93:372–82.
[7] Lahma J, Arkoubi Z, Hejjouji R, et al. About a rare disease misdiagnosed as malignant lymphoma or tuberculosis: Kikuchi-Fujimoto's disease. Pan Afr Med J 2018;31:77.
[8] Kim CH, Hyun OJ, Yoo IeR, Kim SH, Sohn HS, Chung SK. Kikuchi disease mimicking malignant lymphoma on FDG PET/CT. Clin Nucl Med 2007;32:711–2.
[9] Zhang MJ, Xiao L, Zhu YH, Jiang J-j, Jiang M-s, He W. Lymph node uptake of 18F-fluorodeoxyglucose detected with positron emission tomography/computed tomography mimicking malignant lymphoma in a patient with Kikuchi disease. Clin Lymphoma Myeloma Leuk 2010; 10:477–9.
[10] Gotthardt M, Bleeker-Rovers CP, Boerman OC, Oyen WJG. Imaging of inflammation by PET, conventional scintigraphy, and other imaging techniques. J Nucl Med Technol 2013;41:157–69.
[11] Ito K, Morooka M, Kubota K. Kikuchi disease: 18F-FDG positron emission tomography/computed tomography of lymph node uptake. Jpn J Radiol 2010;28:15–9.
[12] Tsujikawa T, Tsuchida T, Imamura Y, et al. Kikuchi-Fujimoto disease: PET/CT assessment of a rare cause of cervical lymphadenopathy. Clin Nucl Med 2011;36:661–4.
[13] Kong E, Chun K, Hong Y, Hah J, Cho I. 18F-FDG PET/CT findings in patients with Kikuchi disease. Nuklearmedizin 2013;52:101–6.
[14] O'Neill D, O'Grady J, Variend S. Child fatality associated with pathological features of histiocytic necrotizing lymphadenitis (Kikuchi-Fujimoto disease). Pediatr Pathol Lab Med 1998;18:79–88.
[15] Yen A, Fearneyhough P, Raimer SS, Hudnall SD. EBV-associated Kikuchi's histiocytic necrotizing lymphadenitis with cutaneous manifestations. J Am Acad Dermatol 1997;36:342–6.
[16] Tsang WY, Chan JK, Ng CS. Kikuchi's lymphadenitis. A morphologic analysis of 75 cases with special reference to unusual features. Am J Surg Pathol 1994;18:219–31.

[17] Dorfman RF, Berry GJ. Kikuchi's histiocytic necrotizing lymphadenitis: an analysis of 108 cases with emphasis on differential diagnosis. Semin Diagn Pathol 1988;5:329–45.
[18] Kuo TT. Kikuchi's disease (histiocytic necrotizing lymphadenitis). A clinicopathologic study of 79 cases with an analysis of histologic subtypes, immunohistology, and DNA ploidy. Am J Surg Pathol 1995;19:798–809.
[19] Lin HC, Su CY, Huang CC, Hwang CF, Chien CY. Kikuchi's disease: a review and analysis of 61 cases. Otolaryngol Head Neck Surg 2003; 128:650–3.
[20] Lin YC, Huang HH, Nong BR, et al. Pediatric Kikuchi-Fujimoto disease: a clinicopathologic study and the therapeutic effects of hydroxychloroquine. J Microbiol Immunol Infect 2019;52:395–401.
[21] Chong Y, Kang CS. Causative agents of Kikuchi-Fujimoto disease (histiocytic necrotizing lymphadenitis): a meta-analysis. Int J Pediatr Otorhinolaryngol 2014;78:1890–7.
[22] Graham LE. Kikuchi-Fujimoto disease and peripheral arthritis: a first!. Ann Rheum Dis 2002;61:475.
[23] Loh JM, Shafi H. Kikuchi-Fujimoto disease presenting after consumption of 'Miracle Mineral Solution' (sodium chlorite). BMJ Case Rep 2014; 2014:bcr2014205832.
[24] Alshammari A, Skoura E, Kazem N, Ashkanani R. Kikuchi disease with generalized lymph node, spleen and subcutaneous involvement detected by fluorine-18-fluorodeoxyglucose positron emission tomography/computed tomography. Mol Imaging Radionucl Ther 2016;25:102–6.
[25] Sumiyoshi Y, Kikuchi M, Ohshima K, Masuda Y, Takeshita M, Okamura T. A case of histiocytic necrotizing lymphadenitis with bone marrow and skin involvement. Virchows Arch A Pathol Anat Histopathol 1992;420:275–9.
[26] Sumiyoshi Y, Kikuchi M, Minematu T, Ohshima K, Takeshita M, Minamishima Y. Analysis of herpesvirus genomes in Kikuchi's disease. Virchows Arch 1994;424:437–40.
[27] Xu LQ, Han YM, Li YW, Sun DB. The clinical and pathological characteristics of histiocytic necrotizing lymphadenitis: analysis of 52 cases. Chin J Intern Med 2006;45:127–9.
[28] Ni LF, Liu XM. Clinical analysis of histiocytic necrotizing lymphadenitis in 68 cases. Natl Med J Chin 2010;90:3147–9.
[29] Murcia Duréndez MJ, Paredes Martínez ML, Navarro Fernández JL, Frutos Esteban L, Claver Valderas MA. Value of (1)(8)F-FDG PET-CT in diagnosis and following of histiocytic necrotizing lymphadenitis (Kikuchi-Fujimotos disease). Rev Esp Med Nucl Imagen Mol 2015; 34:70–2.
[30] Pepe F, Disma S, Teodoro C, Pepe P, Magro G. Kikuchi-Fujimoto disease: a clinicopathologic update. Pathologica 2016;108:120–9.
[31] Du H, Shi Y, Shi Y. Clinicopathologic characteristics and immunophenotypes of histiocytic necrotizing lymphadenitis: an analysis of 84 cases. Chin J Pathol 2016;45:86–90.
[32] Chiu CF, Chow KC, Lin TY, Tsai MH, Shih CM, Chen LM. Virus infection in patients with histiocytic necrotizing lymphadenitis in Taiwan. Detection of Epstein-Barr virus, type I human T-cell lymphotropic virus, and parvovirus B19. Am J Clin Pathol 2000; 113:774–81.
[33] Fu JF, Wang CL, Liang L, Dayan C, Guan-Ping D, Fang H. Kikuchi-Fujimoto disease manifesting as recurrent thrombocytopenia and Mobitz type II atrioventricular block in a 7-year-old girl: a case report and analysis of 138 Chinese childhood Kikuchi-Fujimoto cases with 10 years of follow-up in 97 patients. Acta Paediatr 2007; 96:1844–7.
[34] Jang YJ, Park KH, Seok HJ. Management of Kikuchi's disease using glucocorticoid. J Laryngol Otol 2000;114:709–11.
[35] Yalcin S, Toprak SK, Erismis B, Altundag O, Ozdemir H, Topcuoglu N. Management of Kikuchi-Fujimoto disease using glucocorticoid: a case report. Case Rep Med 2011;2011:230840.